Stress-induced volume reduction of isolated pores in wet soil

Teamrat A. Ghezzehei[1] and Dani Or[2]

Department of Plants, Soils and Biometeorology, Utah State University, Logan, Utah, USA

Received 18 December 2001; revised 8 November 2002; accepted 8 November 2002; published 21 March 2003.

[1] This study deals with deformation of small pores in wet soils of relatively high bulk density such as in the final settlement phase of tilled or disturbed soils. Pore deformation was modeled by volume reduction of spherical voids embedded in a homogenous soil matrix. External constant stress and overburden were considered as steady stresses because the change in interaggregate contact stress under overburden is slow compared to the associated strain rate. In contrast, stress due to passage of farm implements was considered as transient because the rate of change of interaggregate stress is comparable with the strain rate. Rheological behavior of the soil matrix under steady and transient stresses was obtained from independent rheological measurements. Experimental data from the literature were used to illustrate the model. Model predictions of relative density compared favorably with experimental data for constant stress application as well as for constant strain rate experiments. Results showed that the rate of densification decreased as the relative density approached unity (complete pore closure) and the relative stress required for driving densification increased exponentially with increasing relative density. *INDEX TERMS:* 1866 Hydrology: Soil moisture; 1875 Hydrology: Unsaturated zone; 1899 Hydrology: General or miscellaneous; *KEYWORDS:* rheology, stress, strain, pore size, densification, water content

Citation: Ghezzehei, T. A., and D. Or, Stress-induced volume reduction of isolated pores in wet soil, *Water Resour. Res.*, *39*(3), 1067, doi:10.1029/2001WR001137, 2003.

1. Introduction

[2] The structural properties of plow-layer of agricultural soil are in a constant state of change. The loose and unstable structural state that results from tillage gradually evolves to a denser and more stable structure. These changes are accompanied by concurrent changes in soil hydraulic properties, such as soil water retention and hydraulic conductivity. In previous studies, we proposed alternative modeling approaches for posttillage dynamic processes [*Ghezzehei and Or*, 2000, 2001; *Or*, 1996; *Or et al.*, 2000]. These models focused on pore-scale mechanics and addressed soil structural changes induced by internal capillary forces and external steady and transient forces. The underlying concept behind these models was the coalescence of spherical soil aggregates, resulting in growth of the interaggregate contact area and gradual "welding". Discrete representation of soil aggregates as individual units applies to the initial loose state of soil aggregate beds, while adjacent interaggregate contacts are not touching each other (see Figure 1). After attainment of a critical strain value ε_c, adjacent contact regions begin to overlap. Consequently, further deformation involves flow of soil material in a complex pattern toward the center of an enclosed pore that cannot be represented adequately by the radial flow assumed in the contact coalescence model. The purpose of this note is to extend the applications of the contact coalescence model by introducing a complementary geometry that considers volume reduction of pores enclosed in soil. Thus unlike our previous analyses that focused on loose surface soils, the current model is directed toward compaction of dense soils and unconsolidated sediments containing isolated pores.

2. Theoretical Considerations

[3] The basic geometry subsequent to coalescence of individual aggregate contacts beyond the critical strain is that of spherical pores embedded inside a homogeneous matrix of soil. The problem is mathematically similar to deformation of an elastic sphere embedded inside a homogeneous viscous fluid, for which *Fröhlich and Sack* [1946] developed a simple self-consistent model that uses perturbation calculations. The approach was later adapted by *Mackenzie and Shuttleworth* [1949] to modeling closure of isolated pores in the context of free-sintering of ceramic powders. In this note, we use these methods to derive equations of volume reduction for spherical isolated pores embedded in wet soil matrix subjected to omnidirectional stress.

2.1. Geometrical Considerations

[4] We consider a spherical pore of radius r_1 surrounded by a concentric spherical shell of homogeneous (wet) soil with radius r_2, as shown in Figure 2. We consider a uniform stress acting normal to the pore surface defined by

$$P_{oct} = \frac{P_1 + P_2 + P_3}{3}. \quad (1)$$

where P_{oct} is the octahedral stress; and P_1, P_2, and P_3 are stresses acting in the principal directions. From the simple

[1] Now at Lawrence Berkeley National Laboratory, Berkeley, California, USA.

[2] Now at University of Connecticut, Storrs, Connecticut, USA.

0043-1397/03/2001WR001137$09.00

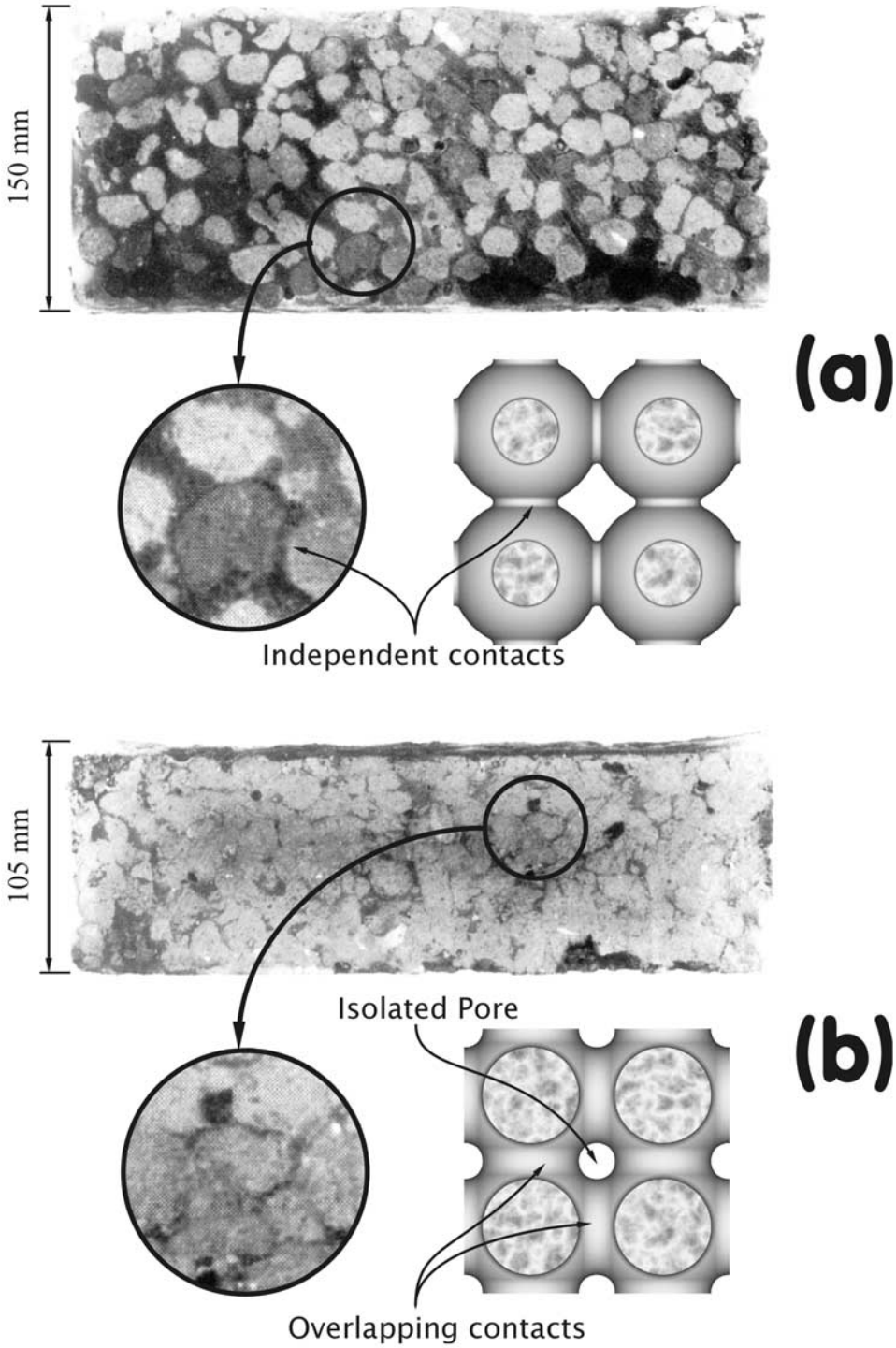

Figure 1. Transition from open pore geometry to closed pore geometry in aggregated soil subjected to axial stress [*Braunack et al.*, 1979]. After the aggregates have been deformed, adjacent interaggregate contacts begin to touch each other. The analogs using the conceptual model of this study are shown.

geometry, we define the relative density of the unit cell relative to the density of the soil material forming the shell as

$$\rho = 1 - (r_1/r_2)^3. \tag{2}$$

[5] The problem at hand is to determine the rate of decrease in pore radius r_1, as determined by the stress, P_{oct}, and the rheology of the soil matrix. The problem is solved by equating the rate of energy dissipation during viscous densification to the rate of work done by reduction of the pore radius [*Frenkel*, 1945].

[6] If the radial velocity of the pore surface is $u_1 = dr_1/dt$, then the radial velocity of the material at any distance r from the origin is $u = u_1 \cdot (r_1/r)^2$, and the radial strain at r is given as

$$\dot{\varepsilon}_r = \frac{du}{dr} = \frac{2 \cdot u_1 \cdot r_1^2}{r^3}. \tag{3}$$

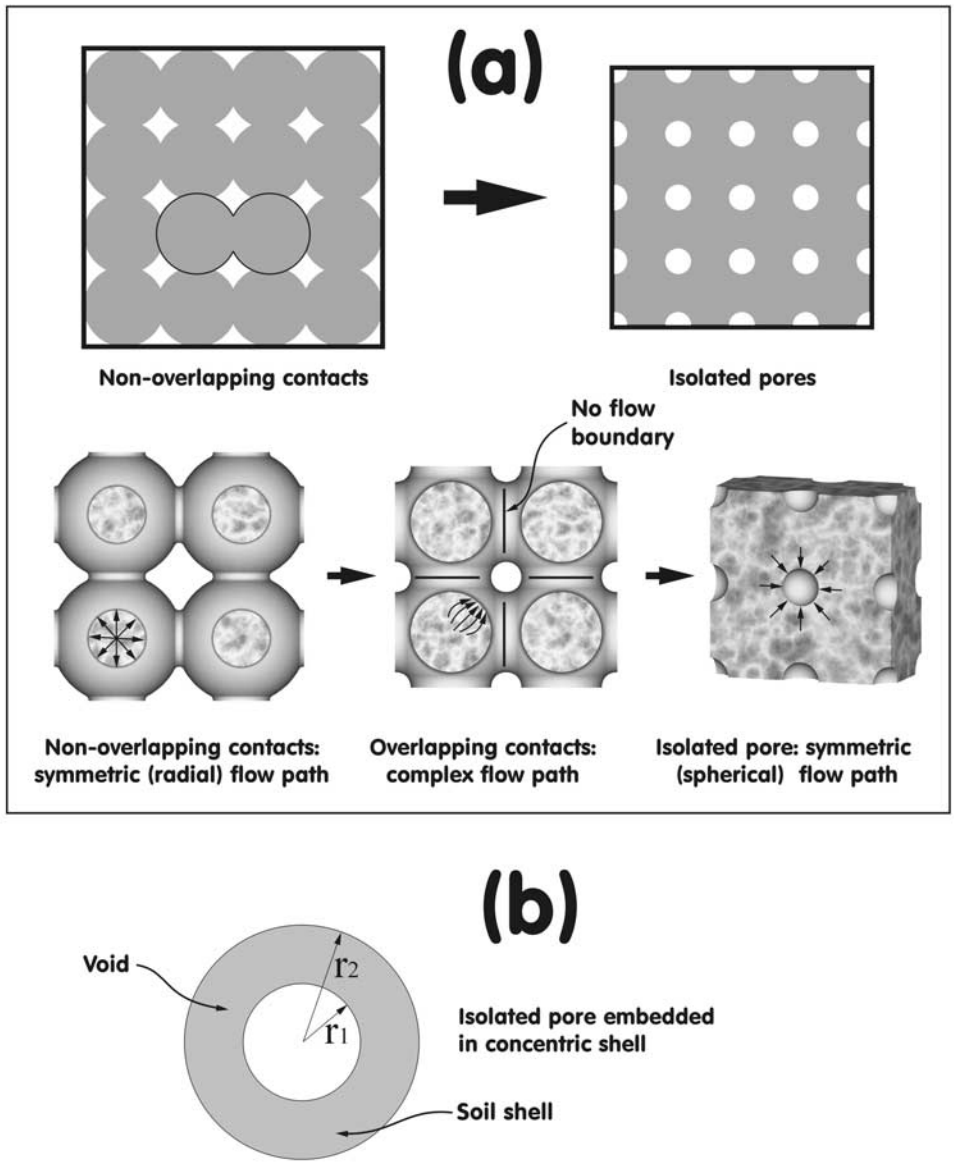

Figure 2. (a) Schematic representation of the transition from open pores to closed pores. Note that for the open pores and closed pores the flow paths are symmetrical, whereas the transition has an asymmetrical complex flow path. (b) Definition of closed pore.

[7] We consider the soil shell as incompressible fluid, with any increase in relative density ρ attributed to decrease in r_1. It follows, then, that the octahedral shear strain rate is [*Mackenzie and Shuttleworth*, 1949]

$$\dot{\gamma} = \sqrt{2} \cdot \dot{\varepsilon}_r \tag{4}$$

2.2. Constitutive Energy Relationships

[8] According to the theory of viscous flow, the rate of energy dissipation in the soil volume between r_1 and r_2 accompanying the pore closure is given as

$$\dot{E}_V = 4 \cdot \pi \cdot \int_{r_1}^{r_2} \left(3 \cdot \dot{\varepsilon}_r^2 \cdot \eta\right) \cdot r^2 dr, \tag{5}$$

where η is viscosity of the soil material in a generic form. The stress, P_{oct}, acting upon the pore surface, $4 \cdot \pi \cdot r_1^2$, does mechanical work at a rate of

$$\dot{\varepsilon}_s = 4 \cdot \pi \cdot r_1^2 \cdot \frac{dr_1}{dt} \cdot P_{oct}. \tag{6}$$

[9] Then, the rate of pore closure can be given in general terms by equating the rate of energy dissipation by viscous flow, $\dot{\varepsilon}_I$, to the rate of mechanical work input, $\dot{\varepsilon}_S$,

$$\frac{dr_1}{dt} = -\frac{3}{r_1^2 \cdot P_{oct}} \int_{r_1}^{r_2} \dot{\varepsilon}^2 \cdot \eta \cdot r^2 dr. \tag{7}$$

[10] Next, we consider two types of stress conditions applicable for agricultural soil dynamics: steady and transient.

2.3. Soil Densification Under Steady Stress

[11] Steady and nondirectional stresses could arise in agricultural soils from, for example, the action of capillary forces during slow drying, and overburden in the subsurface. Under such stress conditions, soil rheology can be described by Bingham viscoplastic model [*Ghezzehei and Or*, 2001],

$$\eta = \eta_p + \tau_y/\dot{\gamma}, \tag{8}$$

where η_p (Pa s) is the coefficient of plastic viscosity, and τ_y (Pa) is the yield stress in shear. Substitution of (2), (4), and (8), into (7) and integrating the right-hand side of (7) yields

$$-\frac{dr_1}{dt} = \frac{P_{oct} r_1}{4\eta_p \rho}\left\{1 + \sqrt{2}\frac{\tau_y}{P_{oct}}\ln[1-\rho]\right\}. \tag{9}$$

Considering that there are n pores per unit volume, each with the volume of $4 \cdot \pi \cdot r_1^3/3$, enables one to derive a direct relationship between the radius of the individual pore and the relative density, ρ and n (m^{-3}),

$$r_1 = \left(\frac{3}{4\pi}\right)^{1/3}\left(\frac{1-\rho}{\rho}\right)^{1/3}\frac{1}{n^{1/3}}. \tag{10}$$

By application of the chain-rule we obtain $u_1 = dr_1/dt = dr_1/d\rho \cdot d\rho/dt$, which, combined with (10), simplifies (9) to

$$\frac{d\rho}{dt} = \frac{3}{4}\frac{P_{oct}}{\eta_p}(\rho - 1)\left\{1 + \sqrt{2}\frac{\tau_y}{P_{oct}}\ln[1-\rho]\right\}. \tag{11}$$

The relative density is obtained by solving (11) with the initial condition $\rho(t_o) = \rho_o$ as

$$\rho(t) = 1 - \mathbf{exp}\left\{-\frac{1}{\sqrt{2}}\frac{P_{oct}}{\tau_y} + \left(\frac{1}{\sqrt{2}}\frac{P_{oct}}{\tau_y} + \mathbf{ln}(1-\rho_o)\right) \cdot \mathbf{exp}\left[\frac{3}{4}\frac{(t_o - t)\sqrt{2}\tau_y}{\eta_p}\right]\right\}. \tag{12}$$

[12] The relative density is plotted as a function of scaled time $(t_o - t)P_{oct}/\eta_p$ for various values of the dimensionless stress P_{oct}/τ_y, as shown in Figure 3. The scaling of the time axis implies that the time required to reach a given soil density is directly proportional to the stress P_{oct} and inversely proportional to the plastic viscosity η_p. The dimensionless stress P_{oct}/τ_y is directly proportional to the maximum density that can be attained at infinite time. For most practical applications, it is sufficient to know the maximum density. This can be explicitly obtained by solving (11) when densification ceases at $d\rho/dt = 0$,

$$\rho_{max} = 1 - \exp\left(-\frac{\sqrt{2}}{2}\cdot\frac{P_{oct}}{\tau_y}\right). \tag{13}$$

[13] The relationship between the stress ratio and the maximum density is depicted in the inset in Figure 3.

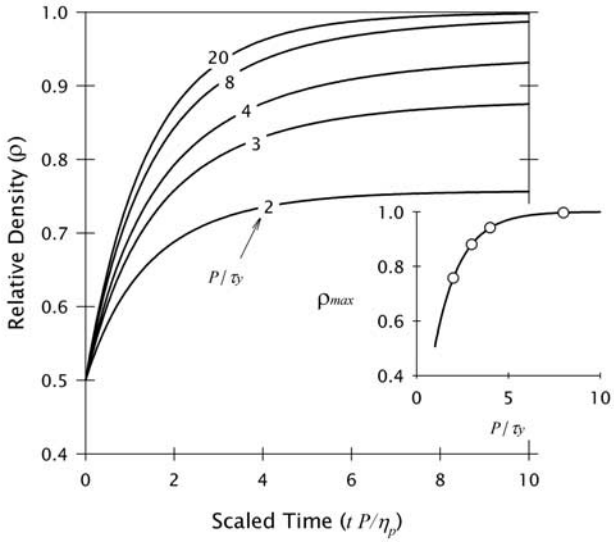

Figure 3. Viscoplastic densification of isolated pore as a function of nondimensional time for various dimensionless load ratios. Inset shows the maximum strain as a function of the dimensionless load ratio (circles denote the load-ratio values used in the main plot).

Equations (12) and (13) imply that either a higher stress or a lower yield stress results in higher maximal density.

2.4. Soil Densification Under Transient Stress

[14] Rheological properties under transient flow conditions are often determined by subjecting a sample to a sinusoidal stress [e.g., *Ghezzehei and Or*, 2001] of the form:

$$\tau = \tau_o\,\mathbf{sin}(\omega t), \tag{14}$$

where τ_o is shear-stress amplitude and ω is angular velocity. The resulting shear strain rate is also sinusoidal:

$$\dot{\gamma} = \gamma_o\omega\,\mathbf{sin}(\omega t + \delta), \tag{15}$$

with $\gamma_o\omega$ being the amplitude of the strain rate and δ is a phase shift angle due to viscous lagging of strain rate path behind the stress path. The ratio of the stress amplitude to the strain rate amplitude defines a complex viscosity term:

$$\eta^* = \frac{\tau_o}{\gamma_o\omega} \tag{16}$$

which can be decomposed into its viscous (energy dissipating) and elastic (energy conserving) components, respectively, as:

$$\eta'' = \eta^*\,\mathbf{sin}(\delta) \tag{17}$$

$$\eta' = \eta^*\,\mathbf{cos}(\delta) \tag{18}$$

[15] Transient stresses in agricultural soil are often induced by passage of farm implements [*Horn et al.*,

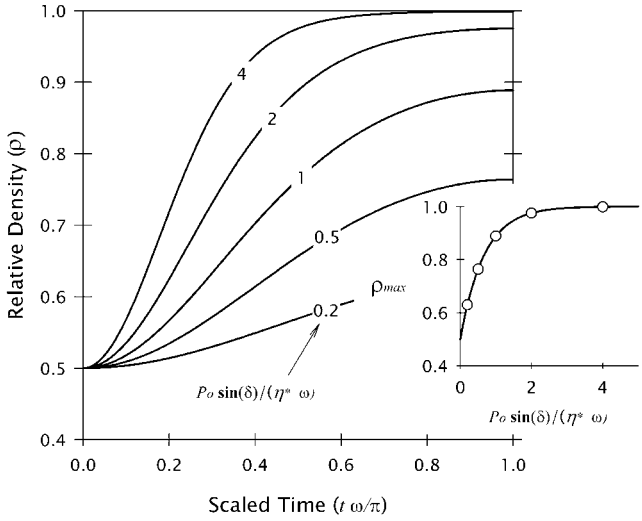

Figure 4. Viscous component of densification resulting from transient stress as a function of nondimensional time for various dimensionless load ratios. Inset shows the maximum strain as a function of the dimensionless load ratio (circles denote the load-ratio values used in the main plot).

1998]. The temporal pattern of such stresses can be approximated by a sinusoidal function,

$$P_{oct} = P_o \,\mathbf{sin}(\omega t), \tag{19}$$

where P_o is amplitude stress. We split the total stress P_{oct} into its viscous and elastic components by assuming linear relationships with $\mathbf{sin}^2(\delta)$ and $\mathbf{cos}^2(\delta)$, respectively:

$$P''_{oct} = P_{oct}\,\mathbf{sin}^2(\delta), \tag{20}$$

$$P'_{oct} = P_{oct}\,\mathbf{cos}^2(\delta), \tag{21}$$

Thus $P''_{oct} = P_{oct}$ for $\delta = 90°$ (perfectly viscous material) and $P'_{oct} = P_{oct}$ for $\delta = 0°$ (perfectly elastic material). The trigonometric identity $\mathbf{sin}^2(\delta) + \mathbf{cos}^2(\delta) = 1$ satisfies the stress closure $P''_{oct} + P'_{oct} = 1$ for all viscoelastic materials $0° < \delta < 90°$.

[16] Because volume reduction of a pore embedded in soil matrix requires flow of material toward the pore, only the viscous component of the stress should play a role in densification. The temporary strain that doesn't involve reduction of the pore (flow of material toward the pore) can be accommodated by temporary deformation of the matrix only. Thus subsequent analyses of densification consider only viscous flow. Upon substituting (20) and (17) for P and η, respectively, in (7) and simplifying we get,

$$\frac{d\rho}{dt} = -\frac{3}{4}\frac{P_o\,\mathbf{sin}(\delta)}{\eta^*}(\rho - 1)\cdot\mathbf{sin}(\omega t). \tag{22}$$

The viscous component of the strain is obtained by integrating (22) after separation of variables, and with the initial condition $\rho(t_o) = \rho_o$,

$$\rho(t) = 1 - (1-\rho_o)\mathbf{exp}\left[-\frac{3}{4}\frac{P_o\,\mathbf{sin}(\delta)}{\eta^*\omega}(1 - \mathbf{cos}(\omega t))\right]. \tag{23}$$

In Figure 4 the solution for time dependent density (23) is evaluated as a function of scaled time $t\omega/\pi$ for various values of dimensionless stress $P_o\mathbf{sin}\,(\delta)/(\eta^*\omega)$. The scaling of the time axis by ω implies frequency dependence of the strain. The maximum density that can be attained for a given frequency depends on the dimensionless stress as shown by the inset in Figure 4. As the relative proportion of the viscous component of the rheological properties increases (increase in sin (δ)) the viscous deformation also increases. Similarly, higher stress and/or low viscosity can be translated to less resistance to flow and result in higher densification.

3. Illustrative Example

[17] The methods presented in this note are illustrated using two examples that compare model predictions with experimental measurements of densification under steady stress.

3.1. Soil Densification Under Steady Stress

[18] In this example, we focus on the ultimate density (13) that results at a given external stress. The model performance is tested by comparison with isotropic compression of modeling clay reported by [*Davis et al.*, 1973]. Equal-sized spheres were formed from modeling clay of plastic consistency. The spheres were arranged in cubic and rhombic packings inside a cylindrical rubber membrane of 100 mm diameter and 100 mm height. The samples were isotropically compressed inside a standard triaxial cell. The volume decrease of the sample in response to applied stress was determined by monitoring the volume of air under constant stress leaving the sample. The relationship between the applied isotropic stress and sample relative density are plotted in Figure 5. *Davis et al.* [1973] scaled the stress by yield stress of the modeling clay determined using frictionless indentation with a sphere. For the subsequent compar-

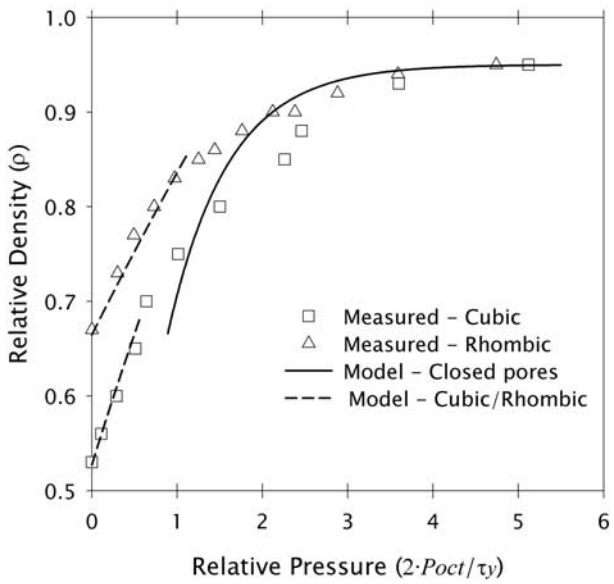

Figure 5. Densification of oil-based modeling clay under isotropic stress for two packing angles, expressed in terms of relative density as a function of dimensionless stress.

isons, we consider the yield stress determined by the indentation experiments to be equivalent to the yield stress in compression, $\sigma_y = \tau_y/2$. Hence the nondimensional stress reported by [*Davis et al.*, 1973] is equivalent to $2 \cdot P_{oct}/\tau_y$. A model given in a companion paper [*Ghezzehei and Or*, 2003] describes the initial densification processes, by coalescence of the spheres at their contacts. The coalescence process is dependent on the packing angles. However, when the pores can be considered as closed (see Figure 1), the initial packing is of no consequence, as the densification process involves only radial flow of material toward the pore center. Ideally, the maximum density of the system is equal to the density of the shell as the pores vanish ($\rho = 1$). However, due to physical constraints, such as air entrapment in isolated pores, this density may not be attained. Hence we adjust the solution (13) to include a maximum relative density that could be less than unity ($\rho_f < 1$)

$$\rho_{max} = \rho_f - \mathbf{exp}\left(-\frac{\sqrt{2}}{2} \cdot \frac{P_{oct}}{\tau_y}\right). \tag{24}$$

[19] In Figure 5, (24) is plotted as a function of the dimensionless stress, with $\rho_f = 0.95$. It describes the post pore-closure processes for both packing angles. At low density, the pore shape is an irregular one enclosed by portions of spheres. At such low densities, the specific pore surface area is less than that of a perfect sphere; hence the rate of work done by the external stress P_{oct} is underestimated. This is, in part, responsible for the underprediction of the density at a load ratio of $2 \cdot P_{oct}/\tau_y \approx 1$.

3.2. Soil Densification Under Constant Strain Rate

[20] In an experimental setup, it is common to compress soil samples under constant strain rate in order to determine stress-strain relationships. The theoretical framework above can be adapted to simulate such experiments. In the simplest case, we consider only one-dimensional densification in the z axis, then the strain ε_z and the relative density of the unit cell ρ are related by,

$$\varepsilon_z = 1 - \rho_o/\rho \tag{25}$$

If the axial strain rate is constant, $d\varepsilon_z/dt = \dot{\varepsilon}_c$, then, by chain rule we have

$$\frac{d\rho}{dt} = \left(\rho^2/\rho_o\right) \cdot \dot{\varepsilon}_c \tag{26}$$

Substituting (26) in (11) gives an implicit relationship between the relative density and the octahedral stress,

$$\frac{\rho^2}{\rho_o}\dot{\varepsilon}_c = \frac{3}{4} \cdot \frac{P_{oct}}{\eta_p}(\rho - 1)\left\{1 + \frac{\sqrt{2} \cdot \tau_y}{P_{oct}} \ln[1 - \rho]\right\} \tag{27}$$

[21] Unlike the previous example, (27) depends on the strain rate, hence time and viscosity are important factors. In this example, we use experimental data of uniaxial compression of a natural soil aggregate bed reported by *Braunack and Dexter* [1978], shown in Figure 6. Different sizes of aggregates of Urrbrae loam (Australia) soil were collected by sieving. The ratio of the major: intermediate: minor axes was 1.0:0.8:0.6 for all the aggregate classes (i.e., resemble spheres). The aggregates were first saturated and then drained to the required matric potential on a pressure plate. The wetted aggregates were packed in a cylindrical compression cell of 80 mm diameter and 100 mm height, and compressed uniaxially at a strain rate of $\dot{\varepsilon}_c = 2.1 \cdot 10^{-4} s^{-1}$. The height of the samples H was recorded as a function of the axial stress P. The stress P was scaled by the tensile yield strength of the individual aggregates Y, measured by the force F required to crush them between parallel plates, and the yield strength was determined by an empirical relationship

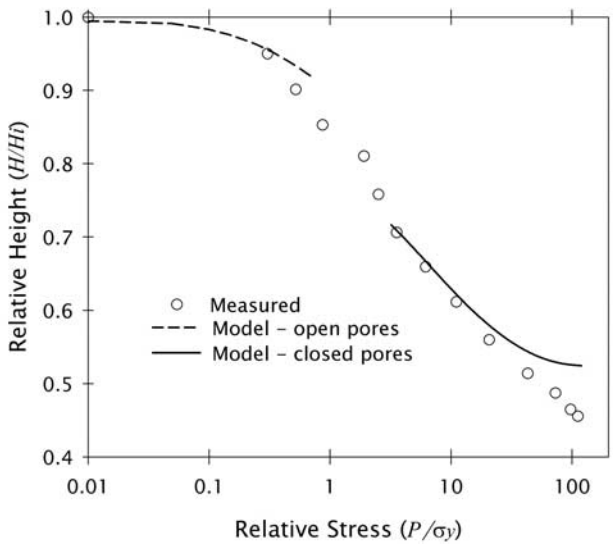

Figure 6. Densification of natural soil aggregates under uniaxial stress at constant strain rate, expressed in terms of relative density as a function of dimensionless stress.

$$Y = 0.576F/d^2, \tag{28}$$

where d is the mean aggregate diameter. For the illustrative comparisons, we assume that the magnitude of yield strength Y is equivalent to σ_y. The data used for this illustrative example was that of 5.1–9.5 mm diameter aggregates at a water content of 0.3 kg kg^{-1} and matric potential of -10 kPa. The tensile yield strength determined by the procedure described above was 21 kPa. In Figure 6, the measured relative sample height (scaled by the initial height $H_i = 100$ mm) is plotted as a function of dimensionless stress P/Y. In view of the large deformations observed in the experimental data, the initial density of the aggregate bed was approximated using cubic packing, that is $\rho_o = 0.524$. The initial deformation, while the interaggregate pores are considered as interconnected, was modeled using the coalescence model.

[22] Because the actual viscosity of soil aggregates was not known, coefficient of plastic viscosity ("ETA"$_p$) was used as a fitting parameter in (27). The value of "ETA"$_p$ that resulted in the best agreement was "ETA"$_p$ = 200 kPa. These comparisons are intended to demonstrate the plausibility of the proposed model. Further experimental work is required for quantitative comparison and model testing.

4. Summary and Conclusions

[23] This study addresses densification of soil with low interaggregate porosity, where models assuming the presence of distinct soil aggregates cannot be applied because of

substantial overlapping of aggregate contact. The objective of this note was to extend the application of the discrete aggregate coalescence models presented in the previous studies [*Ghezzehei and Or*, 2000, 2001, 2003; *Or*, 1996; *Or et al.*, 2000] by considering deformation of relatively dense soils. A self-consistent model that considers volume reduction of spherical pores surrounded by a concentric shell of homogeneous soil matrix was employed. For simplicity, the octahedral mean stress was considered as the driving force for the densification. This implies isotropic volume reduction of the pores, regardless of the anisotropy of the applied external stress. Solutions were provided for densification under steady and transient stress. The scenarios considered for steady stress were: time-dependent density and ultimate density at a constant external stress, and time-dependent densification at a constant strain rate. Under transient stresses, only the viscous part was considered in volume reduction of the spherical pores, whereas, the elastic part was attributed to temporary deformation of the soil matrix surrounding the pores. The geometry of the model is more accurate at higher relative density. The transition zone from coalescence of discrete aggregates to volume reduction of spherical pores is poorly explained by either the aggregate coalescence model or the radial volume reduction model. The application of the models was demonstrated using illustrative examples that compared favorably with measured data from literature. The experimental data, as well as the model calculations, show that the rate of densification decreases as the relative density approaches unity (complete closure of pores), and the relative stress required to drive densification increases exponentially with relative density.

[24] When soils are subjected to uniaxial stresses, such as overburden and traffic, it is likely that soil pores deform anistropically. Consequently the model presented in this note requires further modifications to account for such anisotropic deformation by considering, for example, ellipsoidal pores.

[25] Presently, model calculations are based on a single representative pore. However, the current model is now being extended to interacting ellipsoidal pores [*Eshelby*, 1959; *Mori and Tanaka*, 1973; *Mura and Cheng*, 1977]. Such an extension provides a means for deriving bulk soil-deformation properties such as moduli and Poisson's ratio that are important for relating model calculations with experimental measurements at large sample scales, and provide a link with traditional soil mechanics models. Apart from applications for compaction of agricultural soils, the model could be useful to describe deformation of untilled dense soils, such as for engineering applications.

[26] **Acknowledgments.** The partial funding by USDA/NRI through contract 9700814 and the Research Fund (BARD) through contract 2794-96 is gratefully acknowledged. The work reported herein was performed at Plants, Soils and Biometeorology Department, Utah State University, Logan, Utah.

References

Braunack, M. C., A. R. Dexter, Compaction of aggregate beds, in *Modification of Soil Structure*, edited by W. W. Emerson, R. D. Bond, and A. R. Dexter, pp. 119–126, John Wiley, New York, 1978.

Braunack, M. V., J. S. Hewitt, and A. R. Dexter, Brittle fracture of soil aggregates and the compaction of aggregate beds, *J. Soil Sci.*, *30*, 653–667, 1979.

Davis, P. F., A. R. Dexter, and D. W. Tanner, Isotropic compression of hypothetical and syn-thetic tilths, *J. Terramech.*, *10*, 21–34, 1973.

Eshelby, J. D., The elastic field outside an ellipsoidal inclusion, *Proc. R. Soc. London, Ser. A*, *252*, 561–569, 1959.

Frenkel, J., Viscous flow of crystalline bodies under the action of surface tension, *J. Phys. Moscow*, *9*, 385–391, 1945.

Fröhlich, H., and R. Sack, Theory of the rheological properties of dispersions, *Proc. R. Soc. London, Ser. A*, *185*, 415–430, 1946.

Ghezzehei, T. A., and D. Or, Dynamics of soil aggregate coalescence governed by capillary and rheological processes, *Water Resour. Res.*, *36*(2), 367–379, 2000.

Ghezzehei, T. A., and D. Or, Rheological properties of wet soils and clays under steady and oscillatory stresses, *Soil Sci. Soc. Am. J.*, *65*, 624–637, 2001.

Ghezzehei, T. A., and D. Or, Pore-space dynamics in a soil aggregate bed under a static external load, *Soil Sci. Soc. Am. J.*, *67*(1), 12–19, 2003.

Horn, R., B. G. Richards, W. Grasle, T. Baumgartl, and C. Wiermann, Theoretical principles for modelling soil strength and wheeling effects—A review, *Z. Pflanzen. Bodenk.*, *161*, 333–346, 1998.

Mackenzie, J. K., and R. Shuttleworth, A phenomenological theory of sintering, *Proc. Phys. Soc.*, *62*, 833–852, 1949.

Mori, T., and K. Tanaka, Average stress in matrix and average elastic energy of materials with misfitting inclusions, *Acta Metall.*, *21*, 571–574, 1973.

Mura, T., and P. C. Cheng, The elastic field outside an ellipsoidal inclusion, *J. Appl. Mech.*, *44*, 591–594, 1977.

Or, D., Wetting induced soil structural changes: the theory of liquid phase sintering, *Water. Resour. Res.*, *32*, 3041–3049, 1996.

Or, D., F. J. Leij, V. Snyder, and T. A. Ghezzehei, Stochastic model for post-tillage soil pore space evolution, *Water Resour. Res.*, *36*(7), 1641–1652, 2000.

T. A. Ghezzehei, Lawrence Berkeley National Laboratory, Berkeley, CA 94720, USA. (taghezzehei@lbl.gov)

D. Or, University of Connecticut, Storrs, CT 94720, USA. (dani@engr.uconn.edu)